Chemistry of the $Ag_2(dmb)_2^{2+}$ Template (dmb = 1,8-Diisocyano-*p*-menthane). Preparation, Characterization, and X-ray Structures of the $Ag_2(dmb)_2Y_2$ Dimers (Y = NO_3^-, ClO_4^-, $CH_3CO_2^-$) and the Paramagnetic $[Ag_4(dmb)_4(TCNQ)_3]TCNQ$ Complex (TCNQ = 7,7,8,8-Tetracyanoquinodimethane)

Daniel Fortin,[1a] Marc Drouin,[1b] Pierre D. Harvey,*,†,[1a] F. Geoffrey Herring,[1c] David A. Summers,[1c] and Robert C. Thompson*,[1c]

Département de Chimie, Université de Sherbrooke, Sherbrooke, Québec, Canada J1K 2R1, and Department of Chemistry, University of British Columbia, Vancouver, British Columbia, Canada V6T 1Z1

Received August 13, 1998

Direct reactions of the AgY salts with dmb (1,8-diisocyano-*p*-menthane) in a 1:1 stoichiometric amount generate the binuclear $Ag_2(dmb)_2Y_2$ complexes. The X-ray crystallography establishes that the structure consists of two Ag^+ atoms bridged by two dmb ligands forming a 20-membered ring and by two counteranions via one of the O-atoms, forming a four-membered ring (local symmetry = D_{2h}). The $Ag^I\cdots Ag^I$ separations are 3.909(1) and 3.6831(8) Å for Y = NO_3^- and $CH_3CO_2^-$, respectively. Reactions of $Ag_2(dmb)_2Y_2$ (Y = NO_3^-, ClO_4^-) with LiTCNQ lead to the paramagnetic tetranuclear species $[Ag_4(dmb)_4(TCNQ)_3]TCNQ$. The structure at 180 K consists of two $Ag_2(dmb)_2^{2+}$ species (d(Ag···Ag) = 4.113(1) Å held together by three parallel $TCNQ^-$'s, with $Ag^+\cdots N{\equiv}C$ distances ranging from 2.359(5) to 2.787(5) Å. Two of the Ag^+ atoms are tricoordinated, and the other two are tetracoordinated placed within in a centrosymmetric geometry. The three bridging $TCNQ^-$'s exhibit interplanar distances of 3.333(1) Å, and the Ag_4 species are packed side-by-side with two adjacent $TCNQ^-$'s face-to-face (separation = 3.372(1) Å) forming an infinite π-stacked chain $TCNQ^-$'s. The $TCNQ^-$ counteranion also exhibits weak π-contacts via the −CN groups with other counteranions. The magnetic susceptibilities, EPR spectra, and unit cell parameters have been measured as a function of temperature. The magnetic data are best explained by extended chains of antiferromagnetically coupled $S = {}^3/_2$ and $S = {}^1/_2$ centers for the $[Ag_4(dmb)_4(TCNQ)_3]^+$ and $TCNQ^-$ moieties, respectively. No hyperfine structure has been observed between 106 and 290 K, indicating the presence of rapid exchange in the paramagnetic system. Crystal data: $Ag_2(dmb)_2(NO_3)_2$, crystal system, orthorhombic, space group = C_{cmb}, a = 8.6464(15) Å, b = 16.375(3) Å, c = 20.663(5) Å, Z = 4; $Ag_2(dmb)_2(O_2CCH_3)_2{\cdot}2H_2O$, crystal system triclinic, space group $P\bar{1}$, a = 9.1175(9) Å, b = 9.1451(10) Å, c = 11.7247(8) Å, α = 80.294(7)°, β = 71.124(7)°, γ = 64.258(8)°, Z = 1; $[Ag_4(dmb)_4(TCNQ)_3]TCNQ$, crystal system triclinic, space group = $P\bar{1}$, a = 9.9837(12) Å, b = 13.5194(14) Å, c = 17.1788(9) Å, α = 99.423(6)°, β = 101.512(8)°, γ = 96.917(11)°, Z = 1.

Introduction

The preparation of new materials has become a topic of interest over the past few years.[2] Applications such as conductivity and photoconductivity are still of great interest.[3] Recently our group has taken advantage of the ease with which the dmb ligand forms polymeric materials both in the solid state and solutions, with Ag(I) and Cu(I).[4] More particularly, the $\{[M(dmb)_2]Y\}_n$ polymers (M = Cu, Ag; Y = BF_4^-, PF_6^-, NO_3^-, ClO_4^-, $CH_3CO_2^-$; dmb = 1,8-diisocyano-*p*-menthane), have been prepared and characterized,[4] and as expected, these colorless materials are electrically insulating. One strategy to promote conductivity is to use the well-established tetracyanoquinodimethane (TCNQ) chemistry.[5] The latter exists under the neutral, monoanionic, or polyanionic and mixed-valent forms.[5] For the above polymers, the anion metathesis can easily be performed, but the X-ray diffraction studies reveal that parallel stacking of the planar $TCNQ^-$ species forming an infinite chain does not occur without intercalation of its neutral form.[6] Knowing the very strong tendency of the dmb ligand to form binuclear complexes with Ag(I),[7] Cu(I),[4b] and other metals (Rh, Ni, Ir, Pd, Au),[8] one may consider the use of such species as

* To whom correspondence should be addressed.
† Telephone: (819) 821-7092. Fax: (819) 821-8017. E-mail: pharvey@courrier.usherb.ca.

(1) (a) Université de Sherbrooke. (b) Laboratoire de Chimie Structurale, Université de Sherbrooke. (c) University of British Columbia.
(2) See for examples: (a) Kunkeler, P. J.; van Koningsbruggen, P. J.; Cornelissen, J. P.; van der Horst, A. N.; van der Kraan, A. M.; Spek, A. L.; Haasnoot, J. G.; Reedijk *J. Am. Chem. Soc.* **1996**, *118*, 2190. (b) Gustafsson, G.; Cao, Y.; Treacy, G. M.; Klavetter, F.; Colaneri, N.; Heeger, J. A. *Nature* **1992**, *357*, 477.
(3) (a) Schlureter, J. A.; Geiser, U.; Williams, J. M.; Wang, H.-K.; Kevak, W.-K.; Fendrich, J. A.; Carlson, K. D.; Achenbach, C. A.; Dudek, J. D.; Naumann, D.; Roy, T.; Schirber, J. E.; Bayless, W. R. *J. Chem. Soc., Chem. Commun.* **1994**, 1599. (b) Janssen, R. A. J.; Christiaans, M. P. T.; Hare, C.; Martin, N.; Sariciftei, N. S.; Heeger, A. J.; Wudl, F. *J. Chem. Phys.* **1995**, *103*, 8840.
(4) (a) Perreault, D.; Drouin, M.; Michel, A.; Harvey, P. D. *Inorg. Chem.* **1992**, *31*, 3688. (b) Fortin, D.; Drouin, M.; Turcotte, M.; Harvey, P. D. *J. Am. Chem. Soc.* **1997**, *119*, 531.
(5) Miller, J. S.; Epstein, A. J. *Synthesis and Properties of Low-Dimensional Materials* Annals of the New York Academy of Sciences; New York Academy of Sciences: New York, 1978; Vol. 313.
(6) Fortin, D.; Drouin, M.; Harvey, P. D. *J. Am. Chem. Soc.* **1998**, *120*, 5351.

10.1021/ic980974g CCC: $18.00
Published on Web 03/02/1999

stacking devices. We now wish to report the preparation of new dimeric and tetrameric Ag(I) species based upon the "$Ag_2(dmb)_2^{2+}$" template, and in particular, the preparation of the $[Ag_4(dmb)_4(\mu\text{-}TCNQ)_3]TCNQ$ compound. Although, there are some examples of complexes where $TCNQ^-$ acts as a bridging ligand,[9] the behavior is rather rare.

Experimental Section

Materials. $AgNO_3$, AgO_2CCH_3, and $AgClO_4 \cdot H_2O$ were from Aldrich Chemical Co and were used as received. TCNQ,[10] LiTCNQ,[10] and dmb[11] were prepared according to reported procedures.

Synthesis. $Ag_2(dmb)_2(NO_3)_2$. A 1.3390 g (7.882 mmol) amount of $AgNO_3$ was dissolved in 100 mL of acetonitrile; then 1.500 g (7.882 mmol) of dmb was added. The solution was stirred for 8 h. The solution was reduced to ~20 mL, and diethyl ether was added in order to precipitate the white product. The white solid was filtered, washed with diethyl ether several times, and dried under vaccum; yield > 95%. IR (solid): 2178 (C≡N), 1386 (NO_3) cm^{-1}. ^1H NMR (CD_3CN): δ 1.51 and 1.54 ppm. T_m = 151 °C. The compound was identified from X-ray crystallography; crystals suitable for X-ray crystallography were obtained from slow vapor diffusion of diethyl ether into an acetonitrile solution at room temperature. The compound is light stable.

$Ag_2(dmb)_2(O_2CCH_3)_2$. In 100 mL of a mixture of methanol and water (95:5 (v:v)), 1.316 g (7.882 mmol) of Ag (O_2CCH_3) and 1.500 g (7.882 mmol) of dmb were dissolved and allowed to react for 8 h in the dark under stirring conditions. The solution was concentrated down to ~20 mL under vaccum, before diethyl ether was added (~50 mL). The light-sensitive white precipitate was filtered and washed with diethyl ether. The solid was dried under vaccum. All manipulation was performed in the absence of sun light and in the absence of room light when possible. The compound was also identified by X-ray crystallography; yield > 90%. IR (solid): 2183 (C≡N), 1575 (CO_2) cm^{-1}. ^1H NMR (CD_3CN): δ 1.53 and 1.55 (complex, I = 18, dmb), 1.91 ppm (singlet, I = 3, CH_3CO_2). T_m = 120 °C. Crystals suitable for X-ray crystallography were obtained from slow vapor diffusion of diethyl ether into an acetonitrile solution at room temperature. The crystals were light unstable and were kept in the dark when stored.

$Ag_2(dmb)_2(ClO_4)_2$. In 100 mL of acetonitrile, 1 g (4.438 mmol) of $AgClO_4 \cdot H_2O$ was dissolved and added to 0.845 g (4.438 mmol) of dmb. The solution mixture was stirred gently for 8 h, prior to being evaporated to dryness. The compound was then further dried under vaccum overnight; yield > 95%. Crystallization from acetonitrile/diethyl ether afforded prismatic white crystals as a major product, which differed from the long and narrow needles encountered for the polymeric $\{[Ag(dmb)_2]ClO_4\}_n$ materials. The latter was identified to be a minor impurity (~7%) found by the comparison of the unit cell parameters with an authentic sample. No crystal suitable for X-ray studies was obtained. T_m = 143.5 °C (dec.). IR (solid) = 2186 (C≡N), 1090 cm^{-1} (ClO_4). ^1H NMR (CD_3CN): δ 1.57 and 1.59 ppm (dmb). Anal. Calcd for 93% $Ag_2(dmb)_2(ClO_4)_2$ + 7% $\{[Ag(dmb)_2]ClO_4\}_n$ C, 37.14; H, 4.42; N, 7.31%. Found: C, 37.37; H, 4.81; N, 7.21%. The presence of small amounts of polymers is unavoidable due to the extreme lability of the ClO_4^- anion. *Caution*! Note that any substances containing perchlorate is a potential explosive. They should be handled with care, avoiding strong mechanical shock, or with very small quantities.

$[Ag_4(dmb)_4(TCNQ)_3]TCNQ$. In 250 mL of acetonitrile, 1 g (1.257 mmol) of $Ag_2(dmb)_2(ClO_4)_2$ was dissolved prior to the addition of 100 mL of water. After 10 min, the opaque solution turned clear and 0.531 g (2.514 mmol) of LiTCNQ was added. A green-purple precipitate was formed. The solution was then reduced under vaccum until most of the acetonitrile was evaporated. The precipitate was then filtered and added to 300 mL of methanol, which was kept at boiling for 2 h. The product was then filtered and dried under vaccum; yield > 95%. T_m = 239 °C (dec.). IR (solid) = 2196, 2182, 2167, 2152 cm^{-1} (ν(CN) and ν(NC)). ^1H NMR (CD_3CN): δ 1.50 (18H, dmb), 1.97, 2.07, 2.09 ppm (br, 4H, $TCNQ^-$). Crystals suitable for X-ray crystallography were obtained from a slow vapor diffusion of diethyl ether into a 1:3 (v/v) mixture of DMSO/acetonitrile. The preparation of this same complex can also be performed with $Ag_2(dmb)_2(NO_3)_2$ as a starting material.

X-ray Crystallography. Intensity data were collected on an Enraf-Nonius CAD-4 automatic diffractometer using graphite monochromated Mo Kα radiation. The NRCCAD programs were used for centering, indexing, and data collection. During data collection, the intensities of two standard reflections were monitored every 60 min. The NRCVAX[12] programs were used for absorption correction, data reduction, structure solution, and ORTEP drawings.[13] The SHELXL program was used for structure refinement. The atomic scattering factors stored in SHELXL are from Crowner & Waber (International Tables for X-ray Crystallography, Vol. C, Tables 4.2.6.8 and 6.1.1.4).

Crystal Structure of $[Ag_2(dmb)_2](NO_3)_2$. Intensity data were collected at 193 K. The unit cell dimensions were obtained by a least-squares fit of 24 centered reflections in the range of $20° \le 2\theta \le 25°$. No significant decay (~1%) was observed. A total of 1003 unique reflections was measured, of which 731 were considered to be observed with $I_{net} > 2.5\sigma(I_{net})$. At convergence the final discrepancy indices were R = 0.0434, R_w^2 = 0.0939, S = 1.014. The residual positive and negative electron densities in the final maps were +0.635 and −0.725 e $Å^{-3}$. The dimeric molecule is located on a crystallographic mirror plane, O1 and N2 have *m* symmetry, the Ag atom is located on a 2-fold axis. There is a center of inversion generated by the 2-fold axis perpendicular to the mirror plane in the center of mass of the molecule. The asymmetric unit contains one-fourth of the total molecule. The dmb ligands are disordered. The mirror plane bisects the dmb ligands between C4−C6 and C5 on both sides of the molecule. All H atoms were geometrically placed but not refined. All non-H atoms were refined anisotropically. The disordered atoms were restrained with effective standard deviation to have the same U_{ij} components.

Crystal Structure of $[Ag_2(dmb)_2](CH_3CO_2)_2 \cdot (H_2O)_2$. The experimental procedure is identical to that of $[Ag_2(dmb)_2](NO_3)_2$. The unit cell dimensions were obtained by a least-squares fit of 22 centered reflections in the range of $30° \ge 2\theta \ge 40°$. During data collection, the intensities of three standard reflections were monitored every 60 min. A 12% linear decay was observed after 3 days of data collection. The crystal color changed from white to yellow-orange. A total of 2914 unique reflections was measured, of which 2429 were considered to be observed with $I_{net} > 2.5\sigma(I_{net})$. At convergence the final discrepancy

(7) Perreault, D.; Drouin, M.; Michel, A.; Harvey, P. D. *Inorg. Chem.* **1993**, *32*, 1903.
(8) (a) Perreault, D.; Drouin, M.; Michel, A.; Harvey, P. D. *Inorg. Chem.* **1992**, *31*, 2749. (b) Che, C.-M.; Herbstein, F. H.; Schaefer, W. P.; Marsh, R. E.; Gray, H. B. *Inorg. Chem.* **1984**, *23*, 2572. (c) Gladfelter, W. L.; Gray, H. B. *J. Am. Chem. Soc.* **1980**, *102*, 5909. (d) Rhodes, M.; Mann, K. R. *Inorg. Chem.* **1984**, *23*, 2053. (e) Miskowski, V. M.; Rice, S. F.; Gray, H. B.; Dallinger, R. F.; Milder, S. J.; Hill, M. G.; Exstrom, C. L.; Mann, K. R. *Inorg. Chem.* **1994**, *33*, 2799. (f) Harvey, P. D.; Murtaza, Z. *Inorg. Chem.* **1993**, *32*, 4721. (g) Sykes, A. G.; Mann, K. R. *J. Am. Chem. Soc.* **1988**, *110*, 8252. (h) Sykes, A. G.; Mann, K. R. *J. Am. Chem. Soc.* **1990**, *112*, 7247.
(9) See for examples: (a) Ballester, L.; Barral, M. C.; Gutierrez, A.; Jiménez-Aparicio, R.; Martinez-Muyo, J. M.; Perpignan, M. F.; Monge, M. A.; Ruiz-Valero, C. *J. Chem. Soc., Chem. Commun.* **1991**, 1396. (b) Bartley, S. L.; Dunbar, K. R. *Angew. Chem., Int. Ed. Engl.* **1991**, *30*, 448. (c) Campana, C.; Dunbar, K. R.; Onyang, X. *J. Chem. Soc., Chem. Commun.* **1996**, 2427. (d) Lacroix, P.; Khan, O.; Gleizes, A.; Valade, L.; Cassoux, P. *New. J. Chem.* **1984**, *8*, 643. (e) Humphrey, D. G.; Fallon, G. D.; Murray, K. S. *J. Chem. Soc., Chem. Commun.* **1988**, 1356. (f) Matsumoto, N.; Nonaka, Y.; Kida, S.; Kawano, S.; Veda, I. *Inorg. Chim. Acta* **1979**, *37*, 27. (g) Oshio, H.; Ino, E.; Mogi, I.; Ito, T. *Inorg. Chem.* **1993**, *32*, 5697. (h) Cornelissen, J. P.; van Diemen, J. H.; Goeneveld, L. R.; Harsoot, J. G.; Spek, A. L.; Reedijk, J. *Inorg. Chem.* **1992**, *31*, 198. (i) Ballester, L.; Banal, M. C.; Gutierrrez, A.; Monge, A.; Perpinan, M. F.; Ruiz-Valaro, C.; Sanchez-Pelaez, A. E. *Inorg. Chem.* **1994**, *33*, 2142.
(10) Acker, D. S.; Hertler, W. R. *J. Am. Chem. Soc.* **1962**, *84*, 3370.
(11) Weber, W. P.; Gokel, G. W.; Ugi, I. K. *Angew. Chem., Int. Ed. Engl.* **1972**, *11*, 530.
(12) LePage, Y.; White, P. S.; Gabe, E. J. *NRCCAD, An Enhanced CAD-4 Control Program*, Proceedings of American Crystallographers, Hamilton Meeting; 1986; Abstract PA23.
(13) Johnson, C. K. *ORTEP-A Fortran Thermal Ellipsoid Plot Program*; Technical Report ORNL-5138; Oak Ridge National Laboratory: Oak Ridge, TN, 1976.
(14) Gabe, E. J.; LePage, Y.; Charland, J.-P.; Lee, F. L.; White, P. S. *J. Appl. Crystallogr.* **1989**, *22*, 384.

indices were $R = 0.0387$, $R_w^2 = 0.0983$, $S = 1.025$. The residual positive and negative electron densities in the final maps were +0.752 and −0.633 e Å^{-3}. The dmb ligands are disordered. During the refinement process, the occupancies converge to a 0.596(5)/0.404(5) ratio. We kept the highest occupancy ratio for this work. A water molecule was found in the asymmetric unit and is involved in H-bonding with the complexes in a linear chain fashion via the acetate ligand along the *C* axis.

Crystal Structure of $[Ag_4(dmb)_4(TCNQ)_3]TCNQ$. Intensity data were collected at 180 K. The unit cell dimensions were obtained by a least-squares fit of 24 centered reflections in the range of $30° \geq 2\theta \geq 36°$. No significant decay was observed. An absorption correction was applied on the data based on a ψ-scan measurements on 9 azimuthal reflections. At convergence the final discrepancy indices were $R = 0.0519$ $R_w^2 = 0.1462$, $S = 1.018$. The residual positive and negative electron densities in the final maps were +1.264 and −1.251 e Å^{-3} and were located in the vicinity of the Ag atoms. All non-H atoms were refined anisotropically. The H atoms were geometrically placed but not refined. The dmb ligand was disordered. The occupancy refinement converged to a 0.589(8)/0.411(8) and 0.632(7)/0.368(7) ratio for both dmb.

Magnetic Measurements. Magnetic susceptibilities of a powdered sample were measured over the temperature range 2−300K using a Quantum Design (MPMS) SQUID magnetometer (applied field = 10 000G). A specially designed sample holder, as described previously,[15] was used to minimize the background signal. Magnetic susceptibilities were corrected for diamagnetism of all atoms.[16] A powdered sample for electron paramagnetic resonance (EPR) studies was packed into a quartz glass tube. Spectra were recorded on a Bruker ECS 106 EPR spectrometer. The instrument was equipped with a 50 kHz field modulation. The field sweep was calibrated by Bruker, and the calibration checked with peroxylamine disulfonate. The X-band frequency (~9.8 GHz) was monitored with an EIP model 625A CW microwave counter. Low-temperature measurements to 106 K were performed using a Bruker ER 4112 VT cryostat system.

FAB Mass Measurements. The FAB mass data were obtained on a Kratos MS-50 TCTA spectrometer at the Université de Montréal using an Iontech saddle field source (model FAB 11NF) operating at 70 kV with a 2 mA current. Both thiolglycerol and nitrobenzyl alcohol matrixes were used and gave the same results.

Results and Discussion

Direct reactions between the AgY salts (Y = NO_3^-, ClO_4^-, $CH_3CO_2^-$) and dmb in 1:1 stoichiometric amounts provide the $Ag_2(dmb)_2Y_2$ complexes in good yields. These new crystalline materials are colorless and diamagnetic; properties that are generally expected for the Ag species in the d^{10} electronic configuration. For Y = NO_3^- and $CH_3CO_2^-$, X-ray crystallography (Figures 1 and 2 and Tables 1 and 2) reveals structures consisting of two tetracoordinated Ag atoms bridged by two dmb ligands and two counteranions (local symmetry = D_{2h}). The latter two bridge the metal centers via one O atom only with d(AgO) of 2.485(2) Å for Y = NO_3^- and 2.551(3) and 2.359(3) Å (average = 2.455 Å) for Y = $CH_3CO_2^-$. Such distances indicate a stronger ionic character for the AgO bonds ($r_{cov}(Ag) + r_{cov}(O) = 2.14$ Å; $r_{ion}(Ag^+) + r_{ion}(O^{2-}) = 2.55$ Å),[17] which contrasts with the related $Ag_2(dmb)_2X_2$ species (X = Cl^-, Br^-, I^-),[7] for which the AgX bonds exhibit a stronger covalent character ($r_{ion}(Ag^+) + r_{ion}(X^-) = 2.96$, 3.16, 3.35 Å; $r_{cov}(Ag^+) + r_{cov}(X^-) = 2.41$, 2.58, 2.77 Å; expt = 2.70, 2.80, and 2.92 Å for X = Cl^-, Br^-, and I^-, respectively). As a result, the Ag atoms adopt a strongly distorted tetrahedral geometry,

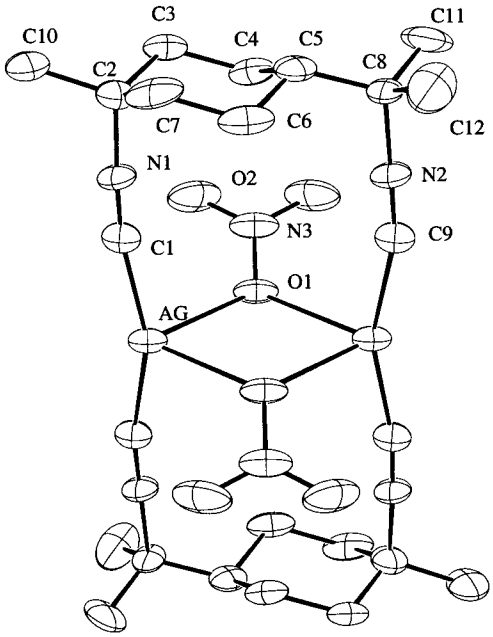

Figure 1. ORTEP drawing for $Ag_2(dmb)_2(NO_3)_2$ with atom labelings. The ORTEP is shown at 30% probability, and the hydrogen atoms are not shown for clarity.

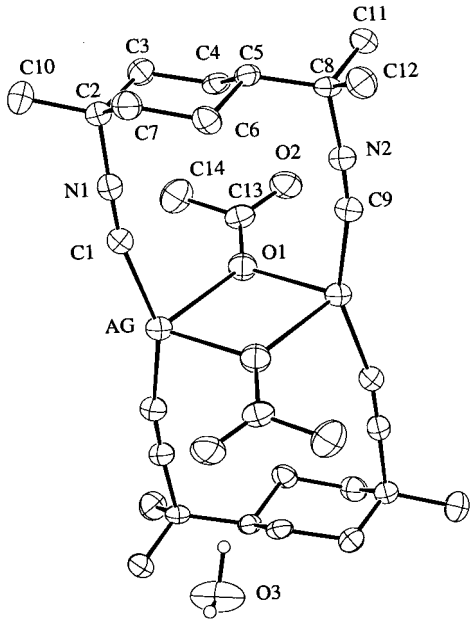

Figure 2. ORTEP drawing for $Ag_2(dmb)_2(CH_3CO_2)_2 \cdot 2H_2O$ with atom labeling. The ORTEP is shown at 30% probability, and the hydrogen atoms are not shown for clarity.

where the ∠CAgC angles significantly deviate from the tetrahedral angle of 109.4° and approach more linear angles (∠CAgC = 156.9(4) and 166.4(6)° for Y = NO_3^-, 153.96(17) for $CH_3CO_2^-$). For the $Ag_2(dmb)_2X_2$ species, this angle ranges from ~143 to 150°.[7] The d(Ag···Ag) values are 3.6832(7) and 3.9075(14) Å for Y = $CH_3CO_2^-$ and NO_3^-, respectively. At such distances, the M_2 interactions are expected to be very weak,[7] and a trend relating these values with the formal charge located on the bridging atom is noted: charge (distance) = −1 (3.345(1) − 3.451(2) Å) < $-1/2$ (3.6832(7) Å) < $-1/3$ (3.9075(14) Å). A literature comparison of the d(Ag···Ag) data for various "Ag(dmb)" complexes is presented in Table 3, and the above values are considered average with respect to halide derivatives (3.345−3.451 Å) and the polymers (4.964−5.1884

(15) Ehlert, M. K.; Rettig, S. J.; Storr, A.; Thompson, R. C.; Trotter, J. *Can. J. Chem.* **1993**, *71*, 1425.
(16) König, E. In *Landolt-Börnstein, New Series*; Hellwege, K. H., Hellwege, A. M., Eds.; Springer-Verlag: Berlin, 1966; Vol. II/2.
(17) Cotton, F. A.; Wilkinson, G.; Gauss, P. L. *Basic Inorganic Chemistry*, 3rd ed.; Wiley: New York, 1995; p 61.

Table 1. Crystallographic Data for Complexes

data	$Ag_2(dmb)_2(NO_3)_2$	$Ag_2(dmb)_2(CH_3CO_2)_2 \cdot 2H_2O$	$[Ag_4(dmb)_4(\mu\text{-TCNQ})_3]TCNQ$
chem formula	$Ag_2C_{24}H_{36}N_6O_6$	$Ag_2C_{28}H_{46}O_6N_4$	$Ag_4C_{96}H_{88}N_{24}$
fw	720.31	750.42	2009.43
space group	C_{cmb}	$P\bar{1}$	$P\bar{1}$
T, K	193	193	180
a, Å	8.6464(15)	9.1176(9)	9.9837(12)
b, Å	16.375(3)	9.1451(10)	13.5194(14)
c, Å	20.663(5)	11.7247(8)	17.1788(9)
α, deg	90.0	80.294(7)	99.423(6)
β, deg	90.0	71.124(7)	101.512(8)
γ, deg	90.0	64.258(8)	96.917(11)
V, Å^3	2925.7(11)	832.8(1)	2213.1(4)
Z	4	1	1
λ, Å	0.710 73	0.710 73	1.541 84
ρ_{calcd}, g cm^{-3}	1.635	1.496	1.508
μ, cm^{-1}	13.8	12.2	74.8
R^a	0.0434	0.0387	0.0519
$R_w{}^{2\,b}$	0.0939	0.0983	0.1462
S^c	1.014	1.025	1.018

[a] $R = \sum(F_o - F_c)/\sum F_o$. [b] $R_w{}^2 = [\sum w(F_o{}^2 - F_c{}^2)^2/\sum(wF_o{}^2)^2]^{1/2}$, $w = 1/[\sigma^2(F_o{}^2) + a(F_o{}^2 + 2F_c{}^2)/3 + b(F_o{}^2 + 2F_c{}^2)/3]$. [c] $S = [\sum(w(F_o{}^2 - F_c{}^2)^2)/(\text{no. of reflcns} - \text{no. of params})]^{1/2}$.

Table 2. Selected Bond Distances (Å) and Angles (deg)

	$Ag_2(dmb)_2(NO_3)_2$	$Ag_2(dmb)_2 \cdot (O_2CCH_3)_2 \cdot 2H_2O$	$[Ag_4(dmb)_4(TCNQ)_3]TCNQ$
d(Ag···Ag)	3.9075(14)	3.6832(7)	4.115(8)
d(Ag−C)	2.084(7)	2.114(4)	2.109(5)
		2.114(4)	2.109(5)
			2.124(5)
			2.128(5)
d(C≡N−)	1.132(11)	1.137(5)	1.133(6)
	1.089(17)	1.133(5)	1.139(6)
			1.145(6)
			1.134(6)
d(Ag−O)	2.485(2)	2.551(3)	
		2.359(3)	
d(Ag···N)			2.500(5)
			2.552(4)
			2.796(4)
			2.361(4)
∠OAgO	76.30(13)	82.87(9)	
∠AgOAg	103.70(13)	97.13(13)	
∠CAgC	156.9(4)	153.96(17)	140.3(2)
	166.4(6)	153.96(7)	147.37(19)
∠AgCN	170.5(11)	166.7(4)	173.8(4)
	162.1(11)	165.7(4)	179.2(5)
			173.2(4)
			174.8(4)

Å). For Y = ClO_4^-, the crystallization of the material afforded white prismatic crystals as a major product (>90% by counting the relative number of crystals) and long and narrow needles. The latter were readily identified to be the $\{[Ag(dmb)_2](ClO_4)\}_n$ polymer from the comparison of the unit cell parameters[4b] and were not investigated further. Chemical analysis indicated that ~7% of the material was the polymer. Attempts to improve this ratio uniformally failed. The FAB mass spectra show a strong peak located at 695, and readily corresponds to $Ag_2(dmb)_2ClO_4$. Additions of free dmb to the dimer lead quantitatively to the polymer.

Direct reactions between the $Ag_2(dmb)_2Y_2$ (Y = ClO_4^-, NO_3^-) and LiTCNQ afford an electrically insulating green-purple material which is identified to be $[Ag_4(dmb)_4(TCNQ)_3]$-TCNQ from X-ray diffraction studies. To our knowledge, this tetranuclear compound is the first example of triple TCNQ bridges between two metal complexes. In this case two $Ag_2(dmb)_2{}^{2+}$ units are held together by three $TCNQ^-$ anions placed parallel to each other in a staircase fashion separated by 3.333(1) Å (Figure 3). Two of the Ag^+ centers are triply coordinated (two isocyanide and one cyano group), and two are tetracoordinated (two isocyanide and two cyano groups; Figures 3 and 4). The triply coordinated Ag^+ centers show the shortest Ag···N distance (d(Ag2···N6) = 2.361(4) Å; d(N6≡C34) = 1.146(6) Å; ∠Ag2···N6≡C34 = 148.6(4)°), while the tetracoordinated Ag^+ atoms show two average Ag···N lengths (d(Ag1···N7) = 2.500(5) Å, d(N7≡C35) = 1.153(7) Å, ∠Ag1···N7≡C35 = 116.6(4)°; d(Ag1···N9) = 2.552(4) Å, d(N9≡C41) = 1.161(6) Å, ∠Ag1···N9≡C41 = 140.8(4)°). The noninteracting Ag/N≡C− groups (Ag2···N9) exhibit a long distance of 2.796(4) Å (∠Ag2···N9≡C41 = 111.2(4)°). The $TCNQ^-$ ligands bridge the Ag^+ centers in a trans-fashion, which is usually the case for the few examples reported in the literature.[9] ∠CAgC's are not linear (∠CAgC = 140.3(2) and 147.37(19)°) and also deviate significantly from ideal 120 and 109.45°. The Ag···Ag separation in the $Ag_2(dmb)_2{}^{2+}$ units is 4.115(8) Å and is significantly longer than that observed in the $Au_2(dmb)(CN)_2$ (3.536(2) Å),[18] $Ag_3(dmb)_2(I)_3$ (3.760(4) and 3.633(4) Å),[19] and $Ag_2(dmb)_2X_2$ complexes (X = Cl^-, Br^-, I^-; 3.345(1)−3.451(1) Å),[7] but shorter than that reported for the polymeric $\{[Ag(dmb)_2Y\}_n$ species (Y = BF_4^-, PF_6^-, NO_3^-, ClO_4^-; 4.9496(1)−5.1884(6) Å).[4a,b] In contrast with $Ag_2(dmb)_2X_2$ species,[7] no weak Ag···Ag interaction is anticipated here.[4] Relevant to this work, the crystal structure of AgTCNQ was reported over 12 years ago by Shields[20] and consists of a polymeric network where TCNQ acts as a tetradentate ligand, and the Ag atoms are tetracoordinated in a distorted tetrahedral fashion. In this case the Ag−N bond distances (2.306(7)−2.346(6) Å)[20] are clearly shorter than that of $[Ag_4(dmb)_4(TCNQ)_3]TCNQ$, indicating the relatively weak bonding of the −C≡N groups with Ag in the tetranuclear compound. In this case, the $Ag_2(dmb)_2{}^{2+}$ moieties readily act as templates.

Table 3. Comparison of the d(Ag···Ag) Data for Various "Ag(dmb)" Complexes

compd	d(Ag···Ag), Å	ref
$Ag_2(dmb)_2Cl_2 \cdot 2CHCl_3$	3.451(2)	7
$Ag_2(dmb)_2Br_2$	3.345(1)	7
$Ag_2(dmb)_2I_2 \cdot CH_3CH_2OH$	3.378(2)	7
$Ag_2(dmb)_2(CH_3CO_2)_2 \cdot 2H_2O$	3.6832(7)	this work
$Ag_2(dmb)_2(NO_3)_2$	3.9075(14	this work
$Ag_3(dmb)_2I_3 \cdot CH_3CH_2OH$	3.760(4)	19
	3.633(4)	
	2.805(4)[a]	
$[Ag_4(dmb)_4(TCNQ)_3]TCNQ$	4.1115(8)	this work
$\{[Ag(dmb)_2]PF_6\}_n$	4.964(1)	4a
$\{[Ag(dmb)_2]BF_4\}_n$	4.9557(9)	4b
$\{[Ag(dmb)_2]ClO_4\}_n$	4.9496(1)	4b
$\{[Ag(dmb)_2]NO_3 \cdot 0.70H_2O\}_n$	5.1884(6)	4b
$\{[Ag(dmb)_2]TCNQ \cdot CH_2Cl_2\}_n$	5.065(8)	6
$Cu_2(dmb)_2I_2 \cdot 2CH_3OH$	3.199(10)	4b
$Au_2(dmb)(CN)_2$	3.536(2)	18

[a] There is no dmb bridge for this bond.

The most striking feature of this structure is that the Ag_4 species stack side-by-side, promoting close contacts between the $TCNQ^-$'s and forming an infinite chain of parallel $TCNQ^-$'s (Figure 4). This intermolecular contact is 3.372 Å and compares favorably to distances found in the charge-transfer dimer $(TCNQ)_2{}^-$ (3.29−3.3 Å) and trimer $(TCNQ)_3{}^{2-}$ (3.24 and 3.39

(18) Che, M.-C.; Wong, W.-T.; Kwong, H.-L. *J. Chem. Soc., Chem. Commun.* **1989**, 243.
(19) Harvey, P. D.; Drouin, M.; Michel, A.; Perreault, D. *J. Chem. Soc., Dalton Trans.* **1993**, 1365.
(20) Shields, L. *J. Chem. Soc., Faraday Trans. 2* **1985**, *81*, 1.

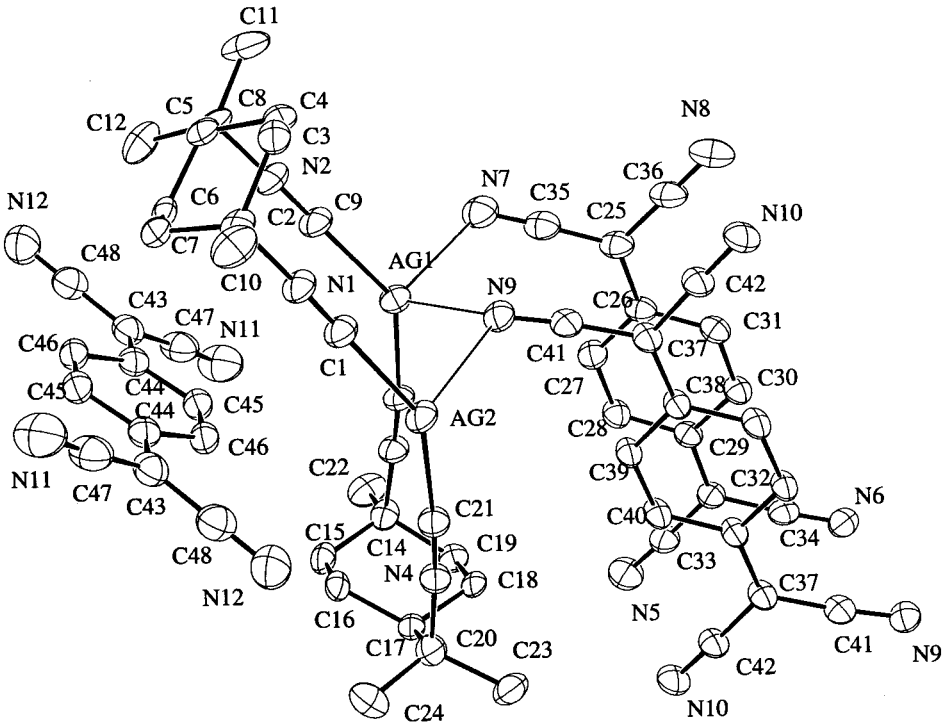

Figure 3. ORTEP drawing and atom labelings for $[Ag_4(dmb)_4(TCNQ)_3]TCNQ$. The ORTEP is shown at 30% probability, and the hydrogen atoms are not shown for clarity. Only half of the molecule is presented since there is a center of inversion in this molecule in the crystal.

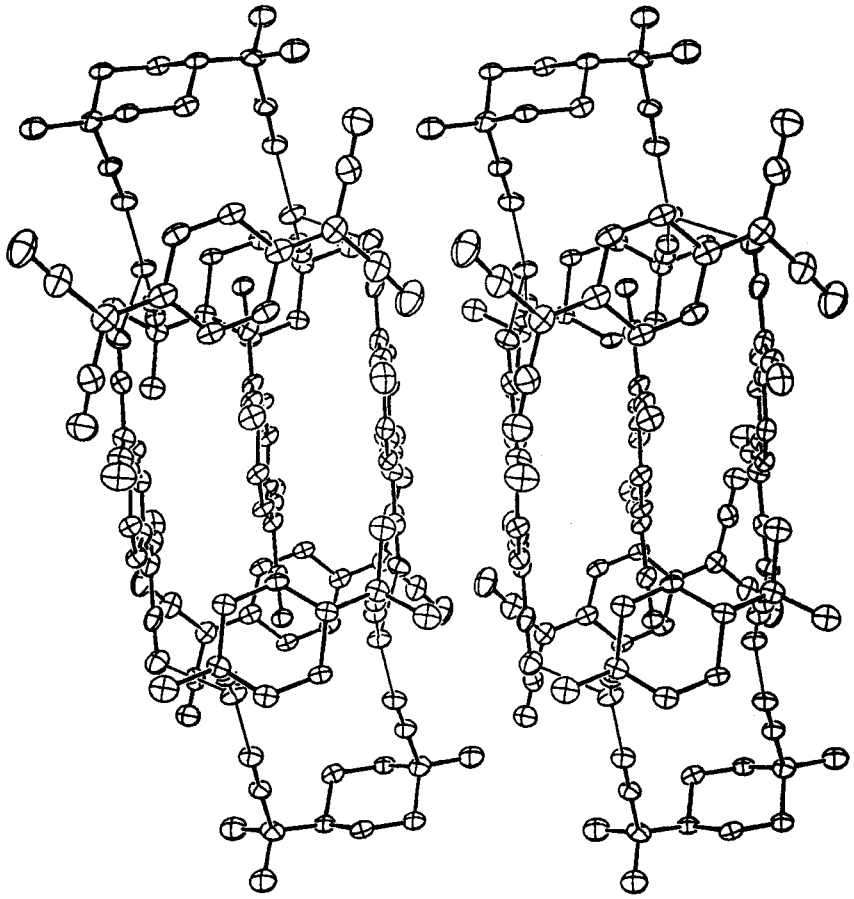

Figure 4. ORTEP drawing for two $[Ag_4(dmb)_4(TCNQ)_3]TCNQ$ with the same conditions described in Figure 3. The two polynuclear complexes are shown side-by-side in order to show the linear packing of the bridging $TCNQ^-$.

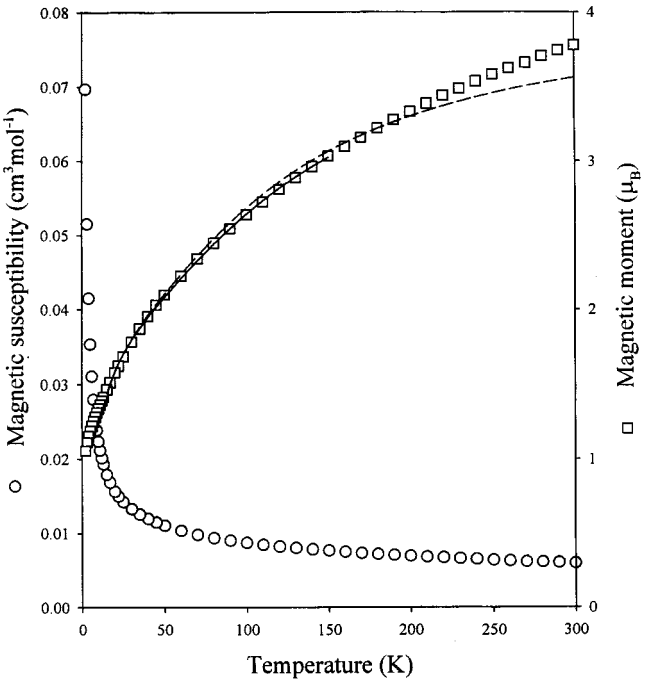

Figure 5. Plots of magnetic susceptibility and magnetic moment versus temperature for $[Ag_4(dmb)_4(TCNQ)_3]TCNQ$. Lines are calculated from theory as described in the text.

Å).[21] Parallel stacking of π-systems at short distances represents the first criteria for electric conductivity.[5] However, while the intramolecular TCNQ···TCNQ contacts between the π-systems are adequate, the overlaps included in the intermolecular interactions are not. Indeed, a slippage of 2.655 Å between the $TCNQ^-$'s is observed, and this infinite chain is in fact better described by an infinite "staircase". As a result, while electronic pairing is possible within the $(TCNQ)_3^{3-}$ fragments, pairing along the infinite staircase is more difficult, so metallic electronic conductivity cannot be easily promoted subsequently (in mixed-valence systems). Thus this structure predicts paramagnetic properties for the odd electron located within the $(TCNQ)_3^{3-}$ fragments, if indeed intermolecular strong coupling does not occur.

The counteranions are clearly placed inside a cavity formed by two $Ag_2(dmb)_2^{2+}$ moieties. However, weak contacts with adjacent counteranionic $TCNQ^-$ are observed where an infinite $\{TCNQ^{-1}\}_n$ chain is formed (d(TCNQ···TCNQ) = 3.26 Å, for the distance between N11 and C47, = 3.33 Å, for the distance between N11 and N11, and = 3.40 Å, for the distance between C47 and C47). These weak interactions occur via the C≡N group of adjacent anions. As such, electronic coupling should be considered to be very weak at this temperature (180 K).

To test the ideas expressed above, the magnetic susceptibilities, EPR spectra, and X-ray unit cell parameters were measured as a function of temperature. Magnetic susceptibility and magnetic moment values over the range 2−300 K are plotted in Figure 5. In interpreting these results, a number of scenarios must be anticipated on the basis of the X-ray structure. First we consider the situation where there is no spin−spin interaction between any of the $TCNQ^-$ groups. This generates four $S = {}^1/_2$ centers per $[Ag_4(dmb)_4(TCNQ)_3]TCNQ$ unit and a predicted magnetic moment of 3.46 μ_B (assuming here and elsewhere that the g factor is 2.00). In the second scenario, on the basis of the crystal structure, we separate the TCNQ groups into (i) the bridging ones that form a three-membered $(TCNQ)_3^{3-}$ unit and (ii) the counteranionic $TCNQ^-$ group. Intramolecular exchange between members of the $(TCNQ)_3^{3-}$ unit can generate a $S = {}^3/_2$ ground state (ferromagnetic coupling) or a $S = {}^1/_2$ ground state (antiferromagnetic coupling). Assuming strong intramolecular coupling and thermal population of the ground states only, the former case would result in a $S = {}^3/_2$ center combined with the $S = {}^1/_2$ from the isolated $TCNQ^-$ and would give a moment of 4.24 μ_B, while in the latter case the $S = {}^1/_2$ plus $S = {}^1/_2$ situation would generate a moment of 2.45 μ_B. Complete intermolecular antiferromagnetic coupling of the counteranionic $TCNQ^-$ groups would leave only the $S = {}^3/_2$ $(TCNQ)_3^{3-}$ units and a moment of 3.87 μ_B, while complete intermolecular antiferromagnetic coupling of the $S = {}^3/_2$ $(TCNQ)_3^{3-}$ units would leave only the $S = {}^1/_2$ $TCNQ^-$ groups and a moment of 1.73 μ_B. Finally complete intermolecular antiferromagnetic coupling of all spin centers would result in a moment of 0 μ_B. These scenarios all represent limiting situations involving spin−spin interactions between the $S = {}^1/_2$ magnetic centers, and, in view of the fact that experiment reveals a magnetic moment per $[Ag_4(dmb)_4(TCNQ)_3]TCNQ$ unit that varies from 3.78 μ_B at 300 K to 1.06 μ_B at 2 K, it is clear that no single scenario adequately describes the situation. We note, qualitatively, that the room-temperature moment is close to that expected for $S = {}^3/_2$ $(TCNQ)_3^{3-}$ units and complete intermolecular antiferromagnetic coupling of the counteranionic $TCNQ^-$ groups, while as the temperature approaches zero the moment approaches that expected for complete intermolecular antiferromagnetic coupling of all spin centers. Attempts at a more detailed analysis of the magnetic properties are described next.

A system involving a linear arrangement of three $S = {}^1/_2$ centers has been treated theoretically, employing a Hamiltonian of the form $H = -2J[S_1S_2 + S_2S_3]$, and the expression for the susceptibility as a function of temperature has been given.[22] In attempting to model our data for $[Ag_4(dmb)_4(TCNQ)_3]TCNQ$, we used this expression to model the $(TCNQ)_3^{3-}$ units and incorporated the expression for the susceptibility of a linear chain of antiferromagnetically coupled $S = {}^1/_2$ centers given by Hiller et al.[23] to model the $S = {}^1/_2$ $TCNQ^-$ groups. While this particular approach did not yield a satisfactory fit to our data, the attempts did indicate that the ground state for the $(TCNQ)_3^{3-}$ units is $S = {}^3/_2$ and not $S = {}^1/_2$ (confirming our earlier qualitative analysis). Moreover these attempts indicated the need to incorporate antiferromagnetic coupling between the $(TCNQ)_3^{3-}$ units in order to better model the experimental data. These observations led to the analysis described below.

The experimental magnetic susceptibility data (on a per mole of $[Ag_4(dmb)_4(TCNQ)_3]TCNQ$ basis) were modeled by employing the expressions for extended linear chains of antiferromagnetically coupled $S = {}^3/_2$ centers (the $(TCNQ)_3^{3-}$ units) and $S = {}^1/_2$ centers (the $TCNQ^-$ groups) as given by Hiller et al.[23] The Hamiltonian is of the form $H = -2J[S_iS_j]$, and the susceptibility expression used is

(21) See for examples for noncoordinated TCNQ: (a) Bell, S. E.; Field, J. S.; Haines, R. J. *J. Chem. Soc., Chem. Commun.* **1991**, 489. (b) Goldberg, S. Z.; Eisenberg, R.; Miller, J. S.; Epstein, A. J. *J. Am. Chem. Soc.* **1976**, *98*, 1976. (c) Lequan, R.-M.; Lequan, M.; Jaouen, G.; Ouahab, L.; Batail, P.; Padiou, J.; Sutherland, R. G. *J. Chem. Soc., Chem. Commun.* **1985**, 116.

(22) Mabbs, F. E.; Machin, D. J. *Magnetism and Transition Metal Complexes*; Chapman and Hall: London, 1973.

(23) Hiller, W.; Strahle, J.; Datz, A.; Hanack, M.; Hatfield, W. E.; ter Haar, L. W.; Gutlich, P. *J. Am. Chem. Soc.* **1984**, *106*, 329.

$$\chi = \frac{Ng^2\mu_B{}^2}{kT}\left[\left[\frac{a + b(|J_1|/kT)^2}{1 + c(|J_1|/kT) + d(|J_1|/kT)^3}\right] + \left[\frac{e + f(|J_2|/kT)^2}{1 + h(|J_2|/kT) + i(|J_2|/kT)^3}\right]\right] \quad (1)$$

where g is the Landé splitting factor, J_1 is the intermolecular exchange coupling constant for the $S = {}^3/_2$ centers, J_2 is that for the $S = {}^1/_2$ centers, and the other symbols have their usual meaning. The coefficients as given by Hiller et al. are as follows: $a = 1.2500$, $b = 17.041$, $c = 6.7360$, $d = 238.47$, $e = 0.2500$, $f = 0.18297$, $h = 1.5467$, and $i = 3.4443$. In examining fits of experimental susceptibilities to eq 1, we fixed g at 2.00 and allowed J_1 and J_2 to vary. In the least-squares fitting procedure used, the following function was minimized:

$$F = \left[\frac{1}{n}\sum_{i=1}^{n}\frac{(\chi_i^{obs} - \chi_i^{calc})^2}{(\chi_i^{obs})^2}\right]^{1/2} \quad (2)$$

Here n is the number of data points. The F value gives a measure of the quality of fit between experiment and theory. We were unable to obtain acceptable fits employing data over the whole temperature range studied. Since traces of paramagnetic impurity can significantly affect the results at low temperatures when the system exhibits overall strong antiferromagnetism, as is the case here, we then examined fits to the data from 15 to 300 K. The agreement between experiment and theory is demonstrated most clearly in the magnetic moment plot shown in Figure 5. The dashed line is calculated from eq 1 with the best-fit values of $|J_1| = 16.6$ cm^{-1} and $|J_2| = 5.8$ cm^{-1} ($F = 0.0452$). The greatest discrepancy between experiment and theory occurs at the higher temperatures. A much better fit was obtained when the data analyzed was limited to the range 15−150 K. The calculated curve for this was obtained with $|J_1| = 17.5$ cm^{-1} and $|J_2| = 5.5$ cm^{-1} ($F = 0.0127$) and is shown as the solid line in Figure 5. One possible explanation of the deviations observed at higher temperatures is that the antiferromagnetic coupling is weaker; that is the $|J|$ values are smaller at these temperatures. That this is, in fact, a reasonable proposition is supported by the measurements made of the unit cell parameters. These studies, to be described in more detail below, show the cell parameters to increase over the 173−293 K temperature range. This increase is presumably accompanied by an increase in intermolecular contacts which, in turn, should result in weaker intermolecular antiferromagnetic exchange. Attempts to fit the higher temperature magnetic data revealed that this could be achieved with smaller values of $|J_1|$ and with $|J_2|$ relatively unchanged. This suggests that the coupling between the $S = {}^3/_2$ centers is more affected by the expansion of the unit cell than is the coupling between the $S = {}^1/_2$ centers. Setting $g = 2.00$ and $|J_2| = 5.5$ cm^{-1}, the value obtained in the fit over the 15−150 K temperature range, and employing eq 1 with $|J_1|$ allowed to vary with temperature, it is possible to obtain complete agreement with each experimental data point at all temperatures above 150 K. Example values of $|J_1|$ required to obtain this agreement are $|J_1| = 17.2$, 16.0, 13.4, and 10.2 cm^{-1} for $T =$ 160, 200, 250, and 300 K, respectively. In summary, the magnetic properties of $[Ag_4(dmb)_4(TCNQ)_3]TCNQ$ may be explained in terms of extended chains of antiferromagnetically coupled $S = {}^3/_2$ and $S = {}^1/_2$ centers. While the magnitude of the exchange between the $S = {}^1/_2$ centers is relatively temperature independent, coupling between the $S = {}^3/_2$ centers appears to weaken as the temperature is increased, particularly over the 150−300 K range.

Table 4. Unit Cell Parameters vs Temperature for $[Ag_4(dmb)_4(TCNQ)_3]TCNQ$

T, K	a, Å	b, Å	c, Å	α, deg	β, deg)	γ, deg)	vol, Å^3
293.15	10.154	13.561	17.274	99.04	101.94	97.68	2264.09
247.65	10.096	13.523	17.238	99.24	101.94	97.47	2240.07
235.75	10.081	13.524	17.232	99.26	101.93	97.30	2237.15
224.05	10.062	13.523	17.224	99.32	101.90	97.18	2232.35
212.15	10.044	13.519	17.219	99.36	101.87	97.08	2227.69
201.85	10.029	13.517	17.212	99.40	101.83	97.00	2223.72
192.55	10.0129	13.515	17.205	99.45	101.80	96.92	2219.13
173.15	9.984	13.519	17.179	99.42	101.51	96.92	2213.09

The EPR spectra exhibit a slightly asymmetric signal exhibiting a g-factor of 2.0019 ± 0.0004 and a width of 2.43 ± 0.05 G. This width is rather large, and no hyperfine structure is observed despite the presence of $^{14}N(I=1)$, $^{1}H(I={}^1/_2)$ and $^{107,109}Ag$ ($I={}^1/_2$). These results indicate that the unpaired electrons are coupled (exchange) along the $TCNQ_n{}^{n-}$ chains which induce the absence of hyperfine coupling. Upon changing the temperature between 106 and 290 K, both the g-factor and bandwidth remain almost the same within the experimental uncertainties, and also no hyperfine coupling is observed. These observations indicate that the odd electrons are still in the exchange process within this temperature range.

The final series of measurements deals with the unit cell parameters as a function of temperature (Table 4). Between 293 and 173 K, all six parameters change as one would predict. Notably the a, b, c parameters decrease by 0.170, 0.042, and 0.095 Å, respectively, within this temperature range. The a axis, which undergoes the greatest perturbation, is the axis parallel to the π-stacking of the $TCNQ^-$ ligands. In other words, the intra- and intermolecular $TCNQ^-\cdots TCNQ^-$ separations vary the most and would be in the order of 3.38 and 3.43 Å, respectively, at room temperature. Such distances well-exceed or are at the upper limit of the separations observed for the charge-transfer species $(TCNQ)_2^-$ (3.29−3.30 Å) and $(TCNQ)_3^-$ (3.24 and 3.39 Å).[21] Upon cooling, these distances gradually and sensitively become shorter. These results corroborate the magnetic moment findings, where $|J_1|$ *must be adjusted* with the change of temperature, with $|J_1|$ decreasing with the increase in unit cell parameters.

Clearly both magnetic and EPR measurements indicate the presence of magnetic exchange and of orbital overlap between the $TCNQ^-$'s. Therefore one can anticipate the possibility of electric conduction for mixed-valence systems. Indeed, the presence of charge transfer along the $TCNQ^-$ 1-D structure is also witnessed by the presence of charge-transfer bands in the low energy region of the electronic spectra.[24] In KBr pellets (at 293 K), typical bands at ∼670 and ∼774 nm are readily observed. Despite the presence of charge transfer as demonstrated by electronic and EPR spectroscopy, this material is an electric insulator, since the conduction band is already filled. One can create a mixed-valence state by adding neutral TCNQ (TCNQ°) to the material, with the hope that the doping TCNQ° will intercalate between the Ag_4 species, keeping this important 1-D structure. To test this hypothesis, the doping of the material with TCNQ° has been performed,[25] and preliminary data

(24) See for instance: Torrance, J. B.; Scott, B. A.; Kaufman, F. B. *Solid State Commun.* **1975**, *17*, 1369.

(25) The doped materials were prepared by dissolving known amounts of TCNQ° and Ag_4 species in acetonitrile. After stirring, and evaporating to dryness, the resulting purple powders were investigated by UV−vis and IR spectroscopy and X-ray powder diffraction pattern and conductivity measurements (four-point probe technique). The materials

indicate that the resulting materials are indeed electrically conducting. The resistivity data show that for a ratio of ~1.20 ($TCNQ^{\circ}/TCNQ^{-}$), the resistivity of the material is 470 Ω cm, a resistivity that is typical for semiconducting materials.

The use of the "$Ag(dmb)^{+}$" species can indeed lead to the design of new magnetic or conducting materials. The preparation of polymeric conducting and photoconducting materials of the type $\{[M(dmb)_2]TCNQ{\cdot}xTCNQ\}_n$ (M = Cu, Ag; x = 0.5, 1.0, 1.5) will be reported in due course.

exhibit more than one different phase, including residuals of the insulating crystals of TCNQ° at high ratios ($TCNQ^{\circ}/TCNQ^{-}$). From UV−vis and IR spectroscopy, clear charge-transfer bands are evident, and coupling between vibrational modes (notably $\nu(C{\equiv}N)$) and the conducting electrons are readily observed.

Acknowledgment. This work was supported by NSERC (Natural Science and Engineering Research Council). P.D.H. also thanks FCAR (Fonds Concertés pour l'Avancement de la Recherche) for funding.

Supporting Information Available: Tables listing crystallographic data, final coordinates and equivalent isotropic thermal parameters, (an-) isotropic thermal parameters, bond distances and angles, and *g*-factor and bandwidth vs temperature and a figure showing the EPR spectrum. This material is available free of charge via the Internet at http://pubs.acs.org.

IC980974G